| Title | Classification of processes for the atomic layer deposition of metals based on mechanistic information from density functional theory calculations |
| --- | --- |
| Authors | Elliott, Simon D.;Dey, Gangotri;Maimaiti, Yasheng |
| Publication date | 2017-02-03 |
| Original Citation | Elliott, S. D., Dey, G.; Maimaiti, Y. (2017) 'Classification of processes for the atomic layer deposition of metals based on mechanistic information from density functional theory calculations', Journal of Chemical Physics, 146(5), 052822 (11pp). doi:10.1063/1.4975085 |
| Type of publication | Article (peer-reviewed) |
| Link to publisher's version | 10.1063/1.4975085 |
| Rights | © 2017, the Authors. Published by AIP Publishing. This article may be downloaded for personal use only. Any other use requires prior permission of the authors and AIP Publishing. The following article appeared in Elliott, S. D., Dey, G.; Maimaiti, Y., Journal of Chemical Physics, 146(5), 052822 (11pp), and may be found at http://dx.doi.org/10.1063/1.4975085 |
| Download date | 2025-08-02 04:33:59 |
| Item downloaded from | https://hdl.handle.net/10468/5750 |

# Classification of processes for the atomic layer deposition of metals based on mechanistic information from density functional theory calculations

S. D. Elliott, G. Dey, and Y. Maimaiti

# Classification of processes for the atomic layer deposition of metals based on mechanistic information from density functional theory calculations

S. D. Elliott,[1,a)] G. Dey,[2] and Y. Maimaiti[1]

[1]*Tyndall National Institute, University College Cork, Lee Maltings, Dyke Parade, Cork T12 R5CP, Ireland*
[2]*Chemistry and Chemical Biology, Rutgers University, 174 Frelinghuysen Road, Piscataway, New Jersey 08854, USA*

Reaction cycles for the atomic layer deposition (ALD) of metals are presented, based on the incomplete data that exist about their chemical mechanisms, particularly from density functional theory (DFT) calculations. ALD requires self-limiting adsorption of each precursor, which results from exhaustion of adsorbates from previous ALD pulses and possibly from inactivation of the substrate through adsorption itself. Where the latter reaction does not take place, an "abbreviated cycle" still gives self-limiting ALD, but at a much reduced rate of deposition. Here, for example, ALD growth rates are estimated for abbreviated cycles in $H_2$-based ALD of metals. A wide variety of other processes for the ALD of metals are also outlined and then classified according to which a reagent supplies electrons for reduction of the metal. Detailed results on computing the mechanism of copper ALD by transmetallation are summarized and shown to be consistent with experimental growth rates. Potential routes to the ALD of other transition metals by using complexes of non-innocent diazadienyl ligands as metal sources are also evaluated using DFT. *Published by AIP Publishing.*
[http://dx.doi.org/10.1063/1.4975085]

## I. INTRODUCTION

Atomic layer deposition (ALD) is a special type of chemical vapor deposition (CVD) by which nanometer-thin films may be grown through the use of sequential, self-limiting reactions.[1,2] The ALD technique is unrivalled in the precision with which film thickness can be controlled at the Å level, without sacrificing uniformity across metre-scale substrates or conformal coating of 3D features. There is much interest in depositing metal films by ALD. Emslie *et al.*[3] review the metals that are deposited through ALD or pulsed CVD and outline the importance of thin films of these metals in current and future technologies. Knisley *et al.* present chemical strategies for the deposition of the first row transition metals.[4] It can be seen that mainly the less electropositive transition metals have been successfully deposited so far.

ALD differs from CVD in that each gas-phase reagent ("precursor") is admitted individually into the reaction zone, with the aim of restricting reactions to the surface only. After transport to the substrate surface, the precursor should adsorb to the surface and react with other moieties already on the surface, generally producing volatile by-products. The defining characteristic of ALD is that, regardless of precursor exposure, at least one of these chemical growth steps is self-limiting under the selected conditions of temperature and pressure, and over the time scale of the experiment. This results in fine control of the amount of film deposited. After purging unreacted gas from the system, the second precursor (or "co-reagent") is admitted and may show similar self-limiting chemistry.

Together, the two precursor pulses form one ALD cycle, which is then repeated so as to grow the desired thickness of the film. Chemical reactivity and inertness at surfaces are thus at the heart of how ALD works. We here report density functional theory (DFT) investigations of the atomic-scale mechanisms of metal ALD chemistry. We are particularly interested in why successful ALD precursors show self-limiting reactivity, and whether the underlying mechanisms can be grouped into classes.

To discuss self-limiting ALD chemistry, it is useful to first consider the prototypical case of oxide ALD: the deposition of $Al_2O_3$ from $Al(CH_3)_3$ and $H_2O$.[5] Figure 1 illustrates the two distinct self-limiting processes that are thought to occur during each precursor pulse in steady-state ALD. In terms of adsorption, $Al(CH_3)_3$ behaves as a strong Lewis acid[6] and therefore, in pulse 1, it adsorbs onto the Lewis basic O sites of the OH-terminated surface, with elimination of ligands as a $CH_4$ by-product, until protons from the surface OH are exhausted (step 1a). This reaction thus self-limits as a result of the fixed coverage of Brønsted acidic $H^+$ in surface OH groups from step 2b. After this, $Al(CH_3)_3$ can still adsorb, without elimination of $CH_4$ (step 1b), until adsorption onto basic surface sites is no longer possible. The adsorption limit could be the result of steric blocking or of electronic deactivation, both of which can affect Lewis adduct formation.[7] The surface is then saturated with a monolayer of Lewis acidic $Al(CH_3)$ and $Al(CH_3)_2$ fragments, and is inert towards further adsorption of $Al(CH_3)_3$. From this viewpoint, we explain the self-limiting nature of ALD by appealing to the saturation of a particular gas-surface chemistry, rather than specifically to surface crowding by adsorbed ligands. On the other hand, this acidic surface is highly reactive towards a Lewis base like $H_2O$,

---

a)Author to whom correspondence should be addressed. Electronic mail: simon.elliott@tyndall.ie
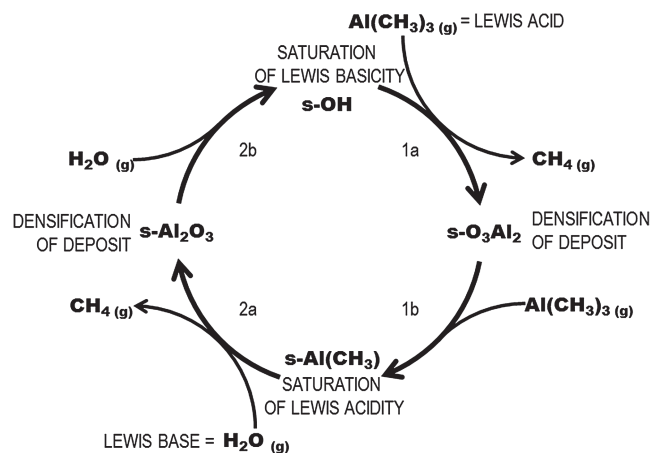
FIG. 1. Schematic ALD cycle at steady state for alumina from trimethyla-luminium (pulse 1, right hand side) and water (pulse 2, left hand side) by acid-base chemistry. "s" refers to the surface and "(g)" to the gas phase. Each pulse is conceptually divided into two steps. Step a shows precursor adsorp-tion that leads to elimination of ligand adducts, until the fragments from the previous pulse are exhausted. Step b shows continued precursor adsorption without elimination, which leads to saturation of the surface with fragments of this precursor.

when pulse 2 begins. Complementary dissociative adsorption and Brønsted elimination reactions can occur until the methyl fragments are exhausted (step 2a), followed by dissociative chemisorption only (step 2b), until the surface becomes too basic for any more $H_2O$ to stick. (Physisorption via H-bonding may occur, but is less likely to lead to oxide growth, as dis-cussed in Reference 8.) We note that steps a and b probably take place simultaneously in each pulse, depending on their kinet-ics relative to surface diffusion; they are shown separately in Figure 1 so as to emphasize that each, separately, can be self-limiting. In this ideal picture, the overall $Al_2O_3$ growth per cycle can be calculated from the amount of each precursor adsorbed, or of by-product eliminated, or from the saturating coverages.

In this paper, we consider whether similar cyclic mech-anisms can account for self-limiting reactions in metal ALD and what growth rates can be expected on the basis of satu-rating coverages. To do this, we review what is known about the mechanisms of metal ALD from atomic-scale calculations, and also present new computed results on growth rate and non-innocent behavior. This allows us to propose a classification of metal ALD processes according to the role of each precursor in the redox process.

Metal-organic complexes are used as metal sources in CVD and ALD because the ligands confer volatility at low temperature. Most commonly, they formally comprise a metal cation surrounded by anionic ligands, so that reduction of the metal center is required for deposition of a metallic film. Elec-trons are thus the "co-reagents" that combine with the metal precursor to yield the target film. Consequently, some pro-cesses use reducing agents as the 2nd precursor (Section III). A major question is then how ligands may be cleanly eliminated, and so we will consider the possibility of some side-reactions that give impurities, such as carbon, or even undesired prod-ucts, such as metal oxide thin films. However, it should be stressed that many more decomposition reactions exist than can be plausibly computed at the requisite level of accuracy.

Alternatively, the ligands of the metal complex can them-selves be the source of electrons, either through decomposition reactions or through variation in their oxidation state (lig-ands that show variable oxidation states are said to behave "non-innocently").[9] In such cases, the 1st (metal) precursor is metastable against reduction and oxidation, and the function of the 2nd (co-reagent) precursor is to trigger the redox process (Section IV). Rather counter-intuitively, oxidizing agents may be used to fulfil the co-reagent role (as in the case of noble metal ALD), which again raises the possibility of depositing an oxide rather than metal.

Our overall goal is to find out whether these two approaches towards redox-based ALD, delivering electrons either from co-reagent or from metastable precursor, are self-limiting. For either source of electrons, the self-limiting nature of ALD ultimately comes down to establishing conditions where precursor adsorption is self-limiting. We therefore begin by examining precursor adsorption onto metal films during metal ALD (Section II).

## II. REDOX ADSORPTION OF METAL PRECURSOR

As noted in Section I, oxide ALD is based on adsorption of a Lewis acidic metal precursor onto Lewis basic surface sites, which enhances the reactivity of the precursor ligands towards subsequent steps. The same Lewis acidic metal pre-cursors are often used for metal ALD, and so in this section we consider whether similar adsorption reactions take place, and what happens to the ligands. We use the example of Cu ALD to illustrate the key concepts. Metal acetylacetonates are frequently used as the precursor for ALD, CVD, and atomic layer etching processes,[10–13] and copper(II) acetylacetonate [Cu(acac)$_2$] has been mainly used in plasma assisted ALD processes to deposit metallic copper and copper oxide. For instance, Wu and Eisenbraun deposited copper thin film on a Ru substrate using Cu(acac)$_2$ and $H_2$ plasmas.[14]

Recently, Hu *et al.* studied the surface chemistry of cop-per metal and copper oxide ALD from Cu(acac)$_2$ and different co-reagents ($H_2$, atomic H and $H_2O$) using periodic DFT and reactive molecular dynamics.[15] The acac ligand remained intact when the adsorbed precursor was exposed to most co-reagents, but atomic H caused the Cu−O and then C−O bonds to break so as to produce $H_2O$ along with ethane, acetone, and methane.

Here, we investigate the effect of the Cu surface during reductive decomposition of Cu(acac)$_2$ via DFT calculations of the adsorption of Cu(acac)$_2$ onto a Cu(111) surface, as a model for step 1b of the ALD process. Details of the method are given in the supplementary material. Figure 2 shows the optimum structure for molecular adsorption and com-pares it with that previously computed for Cu(dmap)$_2$ [dmap = dimethylamino-2-propoxide]. The adsorption energy of the Cu(acac)$_2$ molecule is −2.12 eV. The perpendicular distance between the adsorbate Cu atom and the surface Cu atoms aver-aged over the flat (111) surface is 2.21 Å. Short distances are also observed between ligand C and Cu atoms of the sur-face (2.24 and 2.26 Å), along with distortion out of planarity, indicating formation of new C−Cu bonds and weakening of the conjugated system, including C−O bonds. This supports
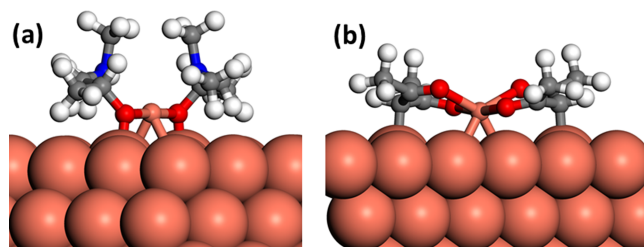
FIG. 2. Computed adsorption structures for Cu(dmap)$_2$ and Cu(acac)$_2$ on Cu(111); colour code: pink = Cu, red = O, blue = N, gray = C, white = H.

the finding of Hu *et al.* that chemisorbed Cu(acac)$_2$ may be reduced in this fashion. Thermal decomposition may therefore, in the absence of H, lead to the deposition of CuO or Cu$_2$O rather than Cu metal. Consistent with this, thermal ALD of copper using Cu(acac)$_2$ has been reported with a three-step process which involves the deposition of the metal oxide and reduction to metal.[16] Ma and Zaera have detected a range of decomposition products when Cu(acac)$_2$ adsorbs: acetylacetone, 3-oxobutanal, Cu(acac)H, acetone, H$_2$, and CO.[17] DFT calculations by Hu *et al.* showed that Cu(acac)$_2$ tends to decompose on the Ta(110) surface.[18] Machado *et al.*[19] have computed that hfac and tmvs ligands decompose on Ta surfaces, leading to deposition of impure Cu, and suggest solving the problem by passivation with a surface nitride.

This may be contrasted with the adsorption of Cu(dmap)$_2$ (Figure 2(a)). It has been found that the adsorption energies and geometries depend on the roughness of the surface and on the method to treat the van der Waals interaction in DFT.[20] Strong distortion of the molecule and cleavage of Cu−N bonds is predicted in the chemisorbed structures, which allows these parts of the ligand to lift off the surface and avoid Cu−C bonding, but also become reactive towards the co-reagent. The molecule gains linear O−Cu−O bonding and this is where charge redistribution with the surface mainly occurs. Bader charge analysis shows that electrons are donated from the surface to the molecule in the chemisorbed structures, so that the Cu center in the molecule is partially reduced and the surface is partially oxidized. Such reduction of the precursor to Ti$^{3+}$ has also been observed by XPS of TiCl$_4$ adsorbing onto metal surfaces.[21]

The same redox behavior is computed to occur during the adsorption of other Cu(II) precursors based on pyrrolylaldehyde N-isopropyl-2-pyrrolylaldiminate and 4N-(ethylamino)pent-3-en-2-onate ligands, as well as acac and dmap.[22] Charge is delocalized between the Cu precursor and the bare copper surface, indicating metallic bonding as the precursor densifies to the surface. It is computed that adsorption is stronger for those precursors with less steric hindrance, flexible ligands, and a planar geometry, because this allows access to surface atoms and the formation of strong metallic bonds. Ligands may dissociate from the adsorbate complex and bond to surface atoms, thus formally oxidizing them to Cu(I). Ligands bound to a layer of Cu(I) atoms are thus predicted to cover the surface after the Cu precursor pulse. Similar ligand dissociation reactions are linked to high rates of metal ALD in the case of cyclopentadienyl-based Ru precursors.[23]

We thus get a picture of metal precursors adsorbing onto the electron-rich metallic surface during step 1b of growth,

with the valence electronic states from the substrate extending over the adsorbate metal atoms, and ligands being transferred to substrate atoms. The net effect is partial oxidation of substrate atoms and reduction of the adsorbate metal centers. The substrate will therefore become saturated with respect to adsorption when its metallicity is exhausted, either through oxidation of surface atoms by the adsorbing metal cation or through steric blocking by redox-inert ligands. Ligands that are redox-active and decompose may lead to other products (e.g., copper oxide).

We therefore expect that electron-rich surface sites are required for adsorption: metals, suboxides, or reducing agents like the hydride anion. This is why the ALD of Co metal from Co(allyl) (CO)$_3$ and dimethylhydrazine (H$_2$NNMe$_2$) is found to proceed selectively on a H-terminated Si surface rather than on OH-terminated SiO$_2$.[24] DFT simulations show that the mechanism involves donation of a H atom (not H$^+$) from the substrate to Co and confirm that this nucleation reaction is thermodynamically favored on Si−H and hindered on SiO$_2$−OH, reflecting the different H-donor capabilities of these surfaces.

## III. CO-REAGENTS AS REDUCING AGENTS

Having established that, at the end of the 1st precursor pulse, pre-existing metal atoms and newly adsorbed metal atoms on the surface are covered with inert ligands and partially oxidized (Section II), it is logical to follow this with a reducing agent as the 2nd precursor, which is the subject of this section. The reducing co-reagent should be strong enough when compared to the reduction potential for generating the target metal from the oxidized surface layer, which may not be the same as the bulk reduction potential.[25] In addition, the remaining ligands should be volatilized by the *in situ* generation of co-reagents such as protons. Clearly, the reducing co-reagent cannot directly and cleanly oxidize an anionic ligand into a single neutral by-product, but may cause ligand decomposition, as discussed for H radicals with acac in Section II. The alternative approach that exploits oxidisable ligands in the 1st precursor is presented in Section IV. A comprehensive discussion of the main families of reducing agents is given by Emslie *et al.*,[3] namely hydrogen gas, main group hydrides, amines or hydrazines, Zn metal, organometallic complexes, and organic molecules (formaldehyde, glyoxylic acid, formic acid, and alcohols). We select two classes of reducing agents for consideration here: hydrogen and organometallic complexes.

### A. Hydrogen as a reducing co-reagent

Hydrogen (H$_2$) can be viewed formally as both a proton donor and hydride donor and so can in principle be used to both eliminate surface-bound ligands (X in Figure 3) and reduce the metal center (step 2a in Figure 3). An alternative description of this chemistry, which Zaera suggests is more appropriate for redox-based ALD, is reductive elimination of ligands by hydrogenation,[26]

$$\text{surf-MX}_n + n/2.\text{H}_{2(g)} \rightarrow \text{surf-M}^{(0)} + n\text{HX}.$$
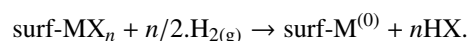
Here, HX may be as simple as a protonated ligand (such as CH$_4$) or may stand for an entire range of reduced by-products.
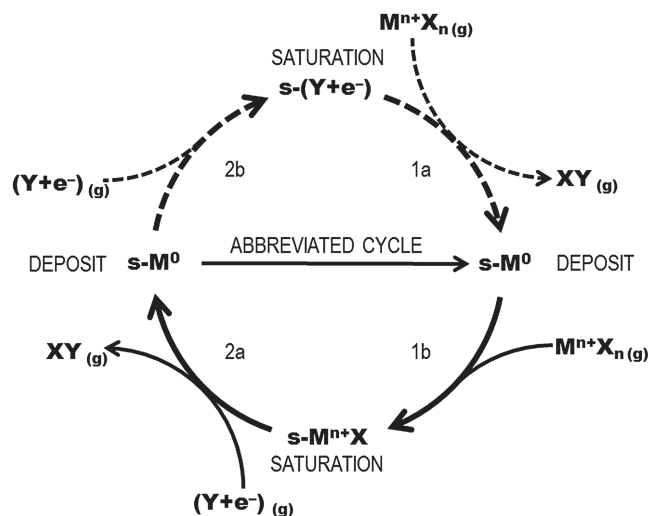
FIG. 3. The schematic mechanistic cycle for a co-reagent as the reducing agent. $MX_n$ is the metal precursor (pulse 1) and $(Y + e^-)$ symbolizes a reducing co-reagent (pulse 2); for example, if $Y = H^+$, then $H = (Y + e^-)$ is a hydrogen radical or half of a $H_2$ molecule. "s" refers to the surface and "(g)" to the gas phase. The dashed arrows indicate uncertainty in steps 2b and 1a and a cycle without these steps is termed "abbreviated."

In either case, this may involve the dissociation of hydrogen gas to yield atomic radicals or (effectively) the hydride anion, and this limits its use to high temperature or plasma ALD processes, or to substrates that catalyze dissociation.[27] (Molecular $H_2$ can, however, be used to reduce oxide-covered surfaces, where these are generated as intermediates on the way to metal ALD.) The reactions of adsorbed H atoms with precursor fragments for Cu ALD were computed in one of the first theoretical studies of any ALD mechanism.[28]

In those cases where a hydride of the target metal is stable, then hydrogen can continue to react and saturate the surface as a hydride (step 2b in Figure 3), which can then go on to reduce the incoming metal precursor in the next cycle. However, not all metals form stable hydrides and so, in general, the hydrogen pulse will terminate when all ligands are eliminated and the surface is entirely reduced to a metal. This means that steps 2b and 1a in Figure 3 will not occur and that the next ALD cycle will begin with molecular or dissociative adsorption of the metal precursor onto the bare surface (step 1b, Section II). (Incidentally, such a bare metal surface is expected to be highly sensitive to gas-phase impurities in the reactor, especially oxygen.) We refer to this as an "abbreviated cycle." Although only one ligand saturates the surface in the abbreviated cycle, the overall growth process is still self-limiting with

respect to both precursors, and is therefore a valid form of ALD.

We now consider what ALD growth rate can be expected for the abbreviated mechanism, using $Cu(acac)_2 + H_2$ as an example. The $Cu(acac)_2$ molecule is computed to chemisorb in a near-planar geometry onto smooth Cu surfaces (Figure 2(b)), covering about 16 Cu atoms of the surface (0.8 nm$^2$). If the acac ligands do not react further in step 1b, then the maximum coverage of such molecules on a surface at the end of step 1b is 1/16 monolayer. Each molecule contains one Cu atom that can contribute to the growth of metallic Cu when hydrogen is introduced in step 2. Bulk layers of Cu are 2.1 Å thick, so that adding 1/16 of a monolayer of Cu in each ALD cycle corresponds to a growth rate of 0.13 Å/cycle.

Reorientation of ligands as they migrate to the surface may allow closer packing and a higher growth rate, while imperfect packing of adsorbates may give a lower growth rate. We therefore estimate that an error margin of ±25% should be applied to the predicted growth rate. The process is limited by the coverage of ligands X, and so the growth rate of M scales inversely with the number of ligands delivered per metal cation, i.e., with the valence of the metal cation. The resulting predictions for maximum growth rates based on these assumptions are given in Table I, along with some cases where the measured growth rates agree reasonably well. Using the correct interlayer spacing for different metals might improve the agreement. It is striking that the predicted growth rates are so low, reflecting the inefficiency of the abbreviated mechanism. As is shown in later parts of this paper, growth rates higher than these limits may indicate that an ALD mechanism with a complete (not abbreviated) cycle is operating. Alternatively, higher rates may signal that reactions are not perfectly self-limiting, which is often described generically as a "CVD component" to growth.

Like hydride, formate can be a source of electrons in metal ALD, as in the three-step ALD process published by Knisley et al. involving the reaction of $Cu(dmap)_2$, HCOOH, and $N_2H_4$.[31] To investigate the mechanism, we suppose that hydrazine dissociates into an $NH_2$ radical in the proximity of an adsorbed formate anion. (We have identified various routes towards the production of reactive $NH_2$, but have not calculated the activation energies that could reveal which route predominates, or whether side-reactions prevent $NH_2$ forming at all.) The calculations show that abstraction of H from the formate anion by $NH_2$ is barrierless and leads to spontaneous decomposition into volatile by-products according to $NH_2 + HCOO^- \rightarrow NH_3 + [COO^-] \rightarrow NH_{3(g)} + CO_{2(g)} + e^-$, with an electron

TABLE I. Predicted growth rates for an "abbreviated cycle" of metal ALD with $H_2$ as the co-reagent, assuming that the metal precursor molecule or its fragments occupies about 1 nm$^2$ of surface area, that no surface hydride forms, and that a metallic layer is 2.1 Å thick.

| System | Predicted growth rate (Å/cycle) | Example | Measured growth rate (Å/cycle) |
|---|---|---|---|
| $M^+X + H_2 \rightarrow M^0$ | 0.26 ± 0.07 | | |
| $M^{2+}X_2 + H_2 \rightarrow M^0$ | 0.13 ± 0.03 | $Cu(thd)_2 + H_2 \rightarrow Cu^0$ | 0.17 at 190-260 °C.[29] |
| $M^{3+}X_3 + H_2 \rightarrow M^0$ | 0.09 ± 0.02 | $Ru(acac)_3 + H_2 \rightarrow Ru^0$ | 0.02-0.07 at 300-370 °C.[30] |
| $M^{4+}X_4 + H_2 \rightarrow M^0$ | 0.07 ± 0.02 | | |

donated directly to the Cu surface as the by-products desorb.[32] We find therefore that hydrazine partially oxidizes formate, which through its complete decomposition to $CO_2$ reduces Cu(I) to $Cu^0$. This illustrates that it is not always straightforward to determine the source of electrons in metal ALD.

## B. Ligand from organometallic co-reagent as the reducing agent

Having discussed $H_2$ as a source of the hydride anion in Sec. III A, we now consider volatile reducing co-reagents where hydride is bound to a metal or semi-metal center: hydrosilanes, hydroboranes, and hydroalanes. An advantage of hydride-based reagents is that, after ligands have been eliminated, these reagents should continue to adsorb and produce a hydride-covered surface (step 2b), which means that the ALD growth rate should be much higher than for the abbreviated cycle of Figure 3. Indeed, the remarkably high growth rate of 1 monolayer/cycle (2.5 Å/cycle) is obtained for probably the best-known such ALD scheme, and also one of the first single-element ALD processes, namely the deposition of tungsten from disilane and $WF_6$.[33] The reactivity of the Si−H surface towards metal ALD was mentioned in Section II.

In a similar vein, many metal alkyls are also strong reducing agents that are volatile. For instance, trimethylaluminium can, through its ligands, reduce oxide substrates in a process known as "clean-up."[34] Trimethylaluminium, triethylborane, and diethylzinc [$ZnEt_2$, where $Et = C_2H_5$] have all been investigated as reducing co-reagents for metal ALD,[35] through the following transmetallation scheme:[36]

$$CuX_{2(g)} + Zn(C_2H_5)_{2(g)} \rightarrow Cu^0_{(s)} + ZnX_{2(g)} + C_4H_{10(g)}.$$
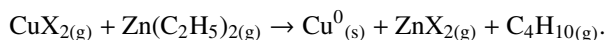
This reaction assumes that there is no change in oxidation state for the ligands X and co-reagent metal Zn, and that the Et ligands become effective reducing agents when they are exchanged onto copper. In order to determine the step-by-step mechanism and possible side-reactions, we carried out DFT calculations, both a wide screening of many ligands and their intermediates,[37] and a detailed consideration of the kinetics of surface reactions[38] at various coverages.[39] We were particularly interested in finding out how the identity of ligand X affects the process, which species saturate the surface, and why co-deposition of Zn is observed to take place.

We found that the order in which surface reactions take place depends on the coverage of ligands on the surface. This is because activation energies are strongly affected by the local environment around a reaction site on the surface. For instance, when $ZnEt_2$ adsorbs onto a surface crowded with CuX fragments, reactions leading to direct desorption of $C_4H_{10}$ are facilitated by the surrounding ligands, which leads to one reaction mechanism. On the other hand, a less-crowded surface favours migration of Et groups to the surface and ultimately desorption of $C_4H_{10}$ from Cu, i.e., a different reaction mechanism. During both mechanisms, ligand diffusion and reordering are generally endothermic processes, which may result in residual ligands blocking surface sites, and cause residual Zn to be reduced and incorporated as an impurity.

In general, the computed data support the overall reaction scheme proposed above.[36] Figure 4 is the cycle of ALD
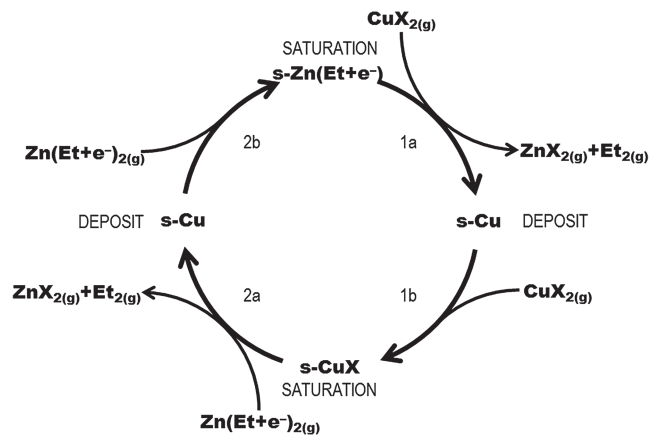


FIG. 4. Schematic mechanistic cycle for metal ALD by transmetallation with co-reagent ligand $Et^- = C_2H_5^-$ as a reducing agent. "s" refers to the surface and "(g)" to the gas phase.

half-reactions that we have determined from the calculations by excluding reaction steps and intermediates that were computed to be too high in energy. It shows that Et groups saturate the surface at the end of the $ZnEt_2$ pulse and thus store electrons on the surface (step 2b). Each $Cu^0$ atom deposited in step 1a is the result of the reductive elimination of two Et groups as butane. Because of the instability of Cu−C bonds, the activation energy for butane formation is lowest when two Et groups have migrated to a single Cu atom,

$$surf\text{-}Cu^{2+}(C_2H_5^-)_2 \rightarrow surf\text{-}Cu^0 + C_4H_{10(g)}.$$
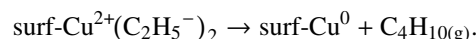
The reaction is therefore limited by the coverage of Et groups at the end of step 2b, which we have estimated[39] at four Et groups per ($6 \times 6$) simulation cell, meaning 2 Cu atoms are deposited per cell. Further adsorption of $Cu(dmap)_2$ is possible in step 1b (for reduction to $Cu^0$ in step 2a), limited by the availability of sufficiently large segments of bare Cu. Our calculations show that adsorption of one $Cu(dmap)_2$ molecule per ($6 \times 6$) cell blocks further adsorption, and this gives a reasonable estimate for the amount of Cu deposited in steps 1b and 2a. This is much less than the contribution to Cu deposition from steps 2b + 1a. The total amount deposited per cycle is therefore three Cu atoms per ($6 \times 6$) cell, or 3/36 of a monolayer. Since the height of one monolayer of crystalline Cu in the (111) direction is 2.10 Å in experiment, the predicted growth rate is 3/36 of this, i.e., 0.18 Å/cycle. This agrees remarkably well with the experimental growth rate of 0.2 Å/cycle,[21] illustrating that the proposed ALD cycle can account for the experimental growth rate.

This is 50% greater than the estimate for abbreviated ALD cycles (Table I, Section II), mostly because of the high coverage of small Et groups storing electrons in step 2b. If metal surfaces can be saturated with even smaller electron sources, such as hydride anions, the metal ALD process is expected to be even more efficient, yielding ALD growth rates that are a multiple of those predicted for the abbreviated cycle. This analysis, therefore, in no way proves that the computed mechanism is correct. However, it does give an indication of how the ALD growth rate is affected by coverages of particular surface intermediates.

## C. Metal from organometallic co-reagent as reducing agent

As noted in Sec. III B, a serious problem with transmetallation is the side reaction of co-deposition of Zn from the co-reagent, because $Zn^{2+}$ is reducible. An alternative approach is to use a co-reagent metal $M^2$ that is *oxidisable*, not reducible, as the reducing co-reagent, along with redox-inert ligands. Such a co-reagent can eliminate ligands from the surface and simultaneously supply electrons for the reduction of the target metal. The by-product complex should be volatile. The desired reaction scheme is

$$M^{n+}X_{n(g)} + n[(M^2)^{m+}Y_m]_{(g)} \rightarrow M^0 + n[(M^2)^{(m+1)+}Y_mX]_{(g)}.$$
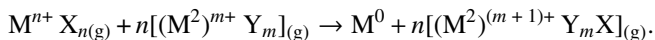
$Y = Cp$ was chosen as a spectator ligand that is usually inert, minimising the danger of C incorporation via ligand decomposition, and low-valent transition metal cations were considered for $M^2$. Redox and desorption energetics from quantum chemical calculations were then used to evaluate the most promising choice of oxidisable metal in a metallocene $M^2Cp_m$.[40] The choice of $M^2$ was found to be the major factor dictating the energetics, with a secondary effect visible due to the identity of the ligands X on the metal precursor that should be transferred to $M^2$. For the example of Cu deposition, vanadocene $[VCp_2]$ was computed to perform best as reducing co-reagent, either stripping oxide or sulfide from a surface, or accepting ligands in the reaction proposed above

$$Cu^{2+}X_{2(g)} + V^{2+}Cp_{2(g)} \rightarrow Cu^0_{(s)} + V^{4+}Cp_2X_{2(g)}.$$
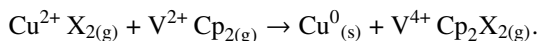
Since vanadocene can be expected to adsorb to a metal surface, steps 2b + 1a of the ALD cycle can be expected to take place, ensuring a high growth rate, limited by the packing of Cp ligands. Experiments in MeOH solution at room temperature demonstrated that Cu metal was deposited by the action of vanadocene on a Cu precursor.[40] Vanadocene may therefore show promise as a gas-phase reducing agent in low-temperature ALD of Cu metal.

## IV. LIGANDS AS REDUCING AGENTS

In this section, we compare various strategies for metal ALD that are all based on one precursor as the source of both metal and electrons, with the electrons originating in the ligands. Such a "single-source" precursor must be metastable against intramolecular redox, being synthesized, stored, and delivered to the reactor intact, but with electron transfer then triggered by reaction with the co-reagent or its fragments at the surface. We identify three cases: (A) release of electrons from the ligands when they bond with the co-reagent; (B) transient generation of an unstable compound at the surface, such as a metal oxide or metal nitride that is itself reducible under the action of the ligands; (C) zero-valent or otherwise "non-innocent" metal precursors.

## A. Ligand-ligand coupling to reduce metal

In this case, the function of the 2nd precursor $M^2Y_n$ is to supply a redox inert bonding partner $Y^-$, which, through to bonding to X, disrupts its electronic structure (formally $X^- \rightarrow X^+ + 2e^-$) and releases two electrons for the reduction of M,

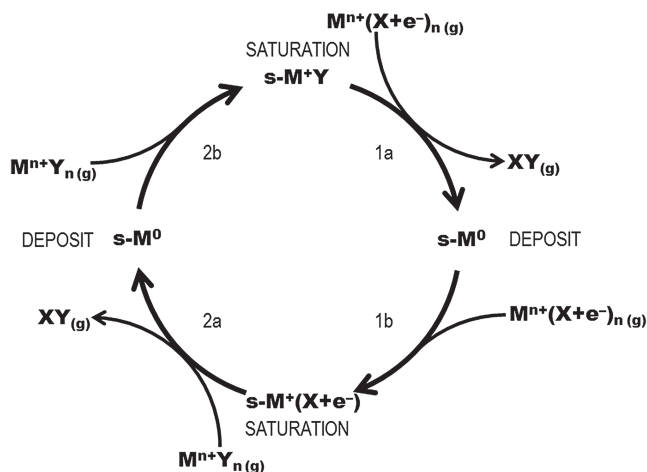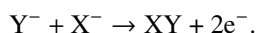$$Y^- + X^- \rightarrow XY + 2e^-.$$



FIG. 5. Cyclic mechanism of metal ALD when both precursors contain the target metal and ligands release electrons when they couple and form a by-product. As shown here, ligand X is redox active and ligand Y is redox inert (Section IV A).

If the by-product XY is volatile, then it is likely that $M^2$ will be reduced and co-deposited, and therefore ALD of pure M may be guaranteed by choosing $M^2 = M$. The likely ALD cycle is illustrated in Figure 5.

Tris(trialkylsilyl)antimony $[(R_3Si)_3Sb, R = Et]$ was used by Pore *et al.* as a platform for ALD of elemental antimony (using $SbCl_3$ as co-reagent) and its compounds (halides of Ge, Te, Ga, or Al as co-reagents).[41] Though antimony is not strictly a metal, the scheme fits well into this section, since formal electron counting suggests that electrons are transferred to Sb from the silyl ligands when the latter bond to the halide and desorb, a reaction termed "dehalosilylation." A conceptually similar reaction was investigated in the solution phase for the deposition of Zn metal from the bishypersilyl complex $Zn(Si(SiMe_3)_3)_2$ and zinc halides, with DFT calculations revealing that reduction takes place through the disruption of high-lying Zn−Si bonding orbitals.[42] Based on this understanding, it was predicted that more volatile non-halide co-reagents, such as $ZnEt_2$, should also be effective,

$$Zn(Si(SiMe_3)_3)_{2(g)} + ZnEt_{2(g)} \rightarrow 2Zn^0_{(s)} + 2Si(SiMe_3)_3Et_{(g)}.$$
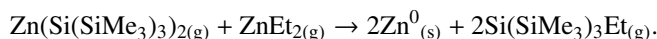
Using a hydrido complex of the target metal as precursor is another way to realize this type of ALD scheme, since the hydride will release electrons when it protonates a redox-inert ligand of the co-reagent. The difficulty lies in stabilizing the metal hydride. We therefore used DFT calculations to propose copper carbene hydride as a precursor for Cu ALD along with any other Cu precursor such as $Cu(dmap)_2$.[43] The advantage of using two Cu precursors is that co-deposition of a second metal cannot occur.

## B. Metal ALD from reducible oxides

By definition, noble metals resist oxidation and their oxides are easily reducible. It was nevertheless surprising when Aaltonen *et al.* discovered that oxygen, oxygen plasma, or ozone could be used as a co-reagent for the ALD of noble metals like Ru[44] and Pt.[45] The likely mechanism is illustrated in Figure 6. The crucial feature of this mechanism is that combustion of hydrocarbon-based ligands by the oxygen co-reagent
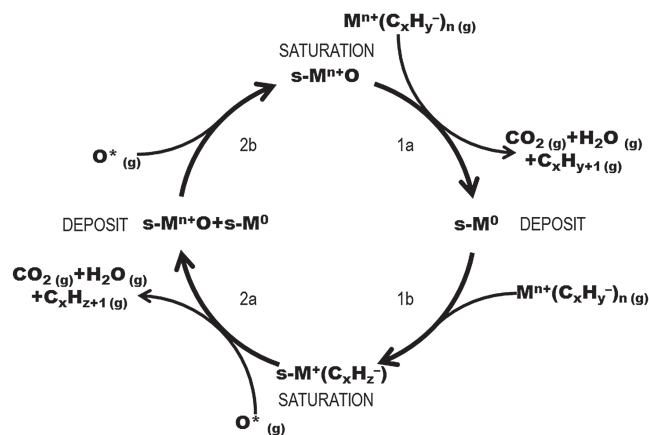
FIG. 6. Cyclic mechanism of metal ALD when a hydrocarbon-based ligand of metal precursor acts as a reducing agent and co-reagent is oxidizing agent such as O-plasma (O*).

not only produces by-products (such as CO, $CO_2$, and $H_2O$) that are volatile, but also transient hydroxyl groups on the surface, which can undergo Brønsted-type elimination of a further ligand (as detected *in situ*[46,47]) or water from the surface (step 2a). Combustion therefore causes each ligand to release one electron for later reduction of the metal. Further oxidation of the surface is self-limiting (step 2b), with the stable thickness of surface oxide characteristic of the particular noble metal. The surface oxide is reducible, and oxidizes the ligands of incoming metal precursors in the next pulse (step 1a), again producing transient OH, electrons, and volatile combustion products. The key process that supplies noble metal atoms (the growth reaction) may thus be described as redox decomposition of the precursor by the metal oxide.[48] After the supply of surface oxygen is exhausted, further adsorption of the metal precursor is probably possible, until the surface is saturated (step 1b).

There are strong parallels with redox reactions in heterogeneous catalysis: while 3 ML is cycled through $Ru^{II}/Ru^0$ in each ALD cycle, only 5% of this is deposited as $Ru^0$, corresponding to the release of one electron from each combusted ligand in the Ru precursor adsorbing at an effective coverage of 0.15 ML. Partial oxidation may account for high growth rates in some experiments (as much as 1.2 or 1.7 Å/cycle).[48]

The end of step 1b during noble metal ALD is probably where the nature of the intermediates saturating the surface is least well characterized. Alkyl ligands are a part of many organometallic precursors for metal ALD, and so it is useful to understand their breakdown on metal substrates, which is also important for a variety of catalytic processes. To this end, Ande *et al.* used DFT to study all possible elementary reactions involved in the interaction of $CH_4$, $C_2H_6$, $C_2H_4$, and $C_2H_2$ with the Ru(0001) surface, and related that to experimental surface science studies.[49] The most stable adsorbed fragments were found to be $Ru-CCH_3$, $Ru-CCH_2$, $Ru-CCH$, and $Ru-CH$, which shows that dehydrogenation is thermodynamically favorable, in agreement with previous experiments. This suggests that the Ru surface becomes saturated with a range of carbonaceous fragments. Dehydrogenation is also observed during ALD processes using copper and manganese

acetamidinate precursors on metal surfaces, leading to bond scission within the acetamidinate ligands.[50]

Recently, a three-step process for the ALD of Au from $(Me_3P)Au(Me)_3 + O_2$-plasma + $H_2O$ has been reported, with the role of $H_2O$ apparently being to remove the $P_2O_5$ co-deposit as volatile $H_3PO_4$ and thus facilitate the auto-reduction of gold oxide to the metal.[51] Since this means a bare metallic surface being produced during the ALD cycle, it is likely that this follows an abbreviated version of Figure 6, with a correspondingly lower growth rate.

## C. Towards zero-valent metal precursors

Ruthenium precursors Ru(EtPh)(R-CHD) with CHD = cyclohexadiene and R = H or R = Et have been described as zero-valent and have been used in conjunction with $O_2$ for the ALD of noble metals.[52] While questions remain over the state of the CHD ligand when coordinated to Ru, the possibility exists that CHD can be eliminated as a neutral molecule, leaving zero-valent Ru. Zero-valent metal precursors would be attractive for ALD. Since the Ru source would not require reduction, the role of the co-reagent would be to remove ligands via oxidation, similar to $O_2$-plasma based ALD of oxides. The oxidation of neutral ligands would not produce transient surface-OH. Growth rates would depend on the coverage of ligands at saturation (step 1b) and on the oxidative capacity of the oxidized surface (step 2b).

Non-innocent ligands are a potential route towards supplying zero-valent metals. Here we present a computational investigation of the potential reactivity of diazadienyl (DAD) complexes of the first row transition metals as a function of identity of the metal and bulk of the ligand. Figure 7 shows the atomic structure of the diazadienyl molecules denoted $R_2DAD$, where R = $^tBu$ for 1,4-di-*tert*-butyl-1,3-diazabutadienyl or R = Me for 1,4-dimethyl-1,3-diazabutadienyl. DAD ligands are also known as $\alpha$-diimines and are analogues of dienes such as CHD. DAD ligands are redox non-innocent, as they can adopt different charge states. Assigning the oxidation states to metal and ligand in a DAD complex is therefore non-trivial. However, it is possible that this non-innocent behavior could be exploited for CVD or ALD, by exchanging the DAD ligands with neutral ligands that force the metal center into zero oxidation state, leading to the deposition of metal.

Knisley *et al.* have described the synthesis, volatility, and thermal stability of DAD complexes of the first row transition metals Cr, Mn, Fe, Co, and Ni, with a view to their use in CVD or ALD.[53] The patent literature includes proposals for the use of Ti diazadienyls as precursors for $TiO_2$ ALD[54] and Cu diazadienyls for Cu ALD.[55] Recently, Klesko, Kerrigan, and Winter reported the use of Co diazadienyl for the
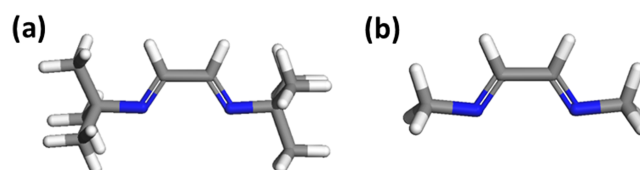


FIG. 7. Stick representations of neutral diazadienyl molecules (a) $^tBu_2DAD$ ($C_{10}H_{20}N_2$) and (b) $Me_2DAD$ ($C_4H_8N_2$); blue = N, gray = C, white = H.

thermal ALD of Co metal using formic acid (HCOOH)[56] or amines (RNH$_2$)[57] as co-reagents. They suggest that the mechanism involves protonation and/or ligand exchange to give a Co complex that then decomposes into Co metal. By contrast, Ni diazadienyl and formic acid apparently yielded Ni oxide, which required a third reagent for reduction to Ni metal.[56] We therefore compute the energetics of exchanging DAD ligands with amines.

We have first computed various charge states of the isolated DAD molecules in the gas-phase using DFT with the PBE0 functional and TZVPP basis set (see the supplementary material). This shows that the neutral and monoanionic forms are close in energy (first electron affinity of tBu$_2$DAD is just −18 kJ/mol), while the dianionic form is substantially less stable (second electron affinity is +454 kJ/mol). Thus, naively considering charge alone, we can propose three possible low-energy redox states for bis-DAD complexes: M$^{II}$(DAD$^-$)$_2$ or M$^I$(DAD$^-$)(DAD$^0$) or M$^0$(DAD$^0$)$_2$, bearing in mind that complexes with the less stable DAD$^{2-}$ dianion may also occur. The calculations also confirm that the bond lengths in the N−C−C−N backbone are sensitive to the redox charge state (computed |C−C| = 148.3 pm, 141.4 pm, and 137.8 pm for neutral, monoanionic, and dianionic forms of free $^t$Bu$_2$DAD, respectively). The C−C bond length can therefore be used to monitor the charge state of the ligand, as previously noted.[58]

It is important to consider electronic spin for a complete description of bonding in DAD complexes. As an example, consider the M$^{II}$(DAD$^-$)$_2$ case. When singly charged, the DAD$^-$ ligand is a radical monoanion with one unpaired electron in an N−C−C−N $\pi$ orbital and an electronic spin of $s = \pm 1/2$. The combined system of two ligands is therefore a biradical triplet with combined ligand spin $S_L = 1$, which would normally be very reactive. In a transition metal complex M(DAD)$_2$ however, these unpaired electrons from the ligand system can couple with the unpaired d electrons of the metal centre (which can have various spin values, $S_M$), to give a total spin $S_{tot} = S_L + S_M$. The coupling can be ferromagnetic, giving a complex with high total spin $S_{tot}$, or antiferromagnetic with low total spin $S_{tot}$, or in-between. This magnetic coupling can be crucial for the stability of the complexes.

The experimentally measured[53] magnetic moments of the $^t$Bu$_2$DAD complexes of Cr, Mn, Fe, Co, and Ni are consistent with antiferromagnetic coupling between ligands and metal in the complex, meaning that the lowest-spin state is obtained. In a simplistic sense, the spin-up electrons on ligand $\pi$ orbitals can be understood as pairing up with some of the spin-down electrons on M:d orbitals. This is a magnetic interaction and should not be interpreted as an electron pair bond between ligands and metal (which would be described as M$^0$(DAD$^0$)$_2$). In fact, $S_{tot}$ of the complex does not uniquely reveal the oxidation states of the constituent metal and ligand ions. Indeed the true situation is even more complex: antiferromagnetic coupling gives a multi-reference ground state, which cannot adequately be described by single electrons in molecular orbitals. Nevertheless, single-reference DFT calculations have been used to give useful approximate information about DAD complexes[59] and here we present DFT results on the oxidation state, structure, and reactivity of these complexes.

The computed structures lead us to assign the M(III) oxidation state to the Ti, V, and Cr complexes because of back-bonding from occupied M:d orbitals into empty ligand $\pi$ orbitals. The Mn, Fe, Co, and Ni diazadienyls have very similar structure (Figure 7) and are assigned the M(II) state (see the supplementary material). Cu(DAD)$_2$ has too few unpaired electrons on the metal center for antiferromagnetic coupling, and so is computed to be particularly unstable.

As can be seen in Figure 8, the bulky bidentate $^t$Bu$_2$DAD ligands are constrained to coordinating to the metal center in a distorted tetrahedral arrangement. We therefore investigated whether this steric constraint could be masking a Jahn-Teller distortion, via evaluating the energy difference for the replacement of $^t$Bu with Me groups in the DAD ligands, i.e., M($^t$Bu$_2$DAD)$_2$ + 2(Me$_2$DAD) → M(Me$_2$DAD)$_2$ + 2($^t$Bu$_2$DAD). We found that in Cr($^t$Bu$_2$DAD)$_2$ the ligating N atoms are disposed about Cr(III) in a distorted D$_{2d}$ tetrahedron, but replacement of $^t$Bu with Me releases 58 kJ/mol of strain energy and produces a near-planar Cr(Me$_2$DAD)$_2$ complex. Similar frustration of Jahn-Teller distortion is evident in the $^t$Bu$_2$DAD complexes of Ni(II) (86 kJ/mol) and Cu(II) (23 kJ/mol) and it may be possible to exploit this built-in strain by favoring ligand elimination in an ALD or CVD process. The Mn, Fe, and Co complexes have strain energies <10 kJ/mol and show no Jahn-Teller distortion.

We now compute the reactivity of the DAD complexes with respect to ligand exchange reactions that are representative of ALD processes. In an actual deposition situation, the relevant exchange reaction would occur at a surface. However, we use a gas-phase model and propose that the computed energetics are a good description of those of the corresponding surface reaction, as long as the electronic state in the gas-phase complex is similar to that of adsorbed M. This is an open question, as adsorption to a surface may change the oxidation state of the metal (see Section II). Details of the method for
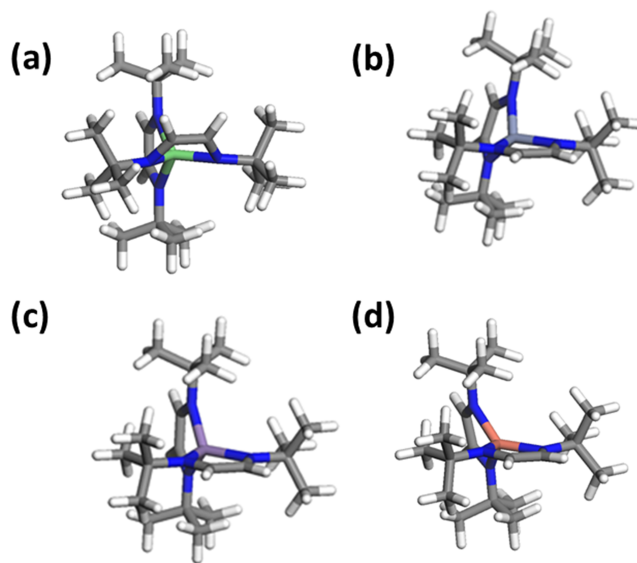


FIG. 8. The computed structures of low-spin M($^t$Bu$_2$DAD)$_2$ complexes: (a) M = Ti(III) and V(III) have the same structure with one "bent" ligand and one "end-on" ligand each, (b) M = Cr(III), (c) M = Mn(II), Fe(II), Co(II), and Ni(II) have the same structure, (d) M = Cu(II); blue = N, gray = C, white = H.

TABLE II. Computed data for M($^t$Bu$_2$DAD)$_2$ complexes: $S_{tot}$ from computed spin; formal oxidation state and electronic configuration of M based on |C–C| distances; reaction energy $\Delta E(1)$ for replacing 2DAD ligands with $n$(CO) ligands; reaction energy $\Delta E(2)$ for replacing 2DAD$^-$ ligands with 2(NMe$_2$$^-$). $m$(NMe$_3$) in the M(II) complexes, with * marking the absence of comparable data for M(III) complexes.

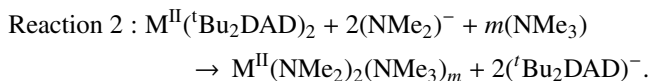| M | Ti | V | Cr | Mn | Fe | Co | Ni | Cu |
|---|---|---|---|---|---|---|---|---|
| $S_{tot}$ of low spin state of M(DAD)$_2$ | 0 | 0.5 | 1.0 | 1.5 | 1.0 | 0.5 | 0 | 0.5 |
| Oxidation state of M | III | III | III | II | II | II | II | II |
| Electronic configuration of M | d$^1$ | d$^2$ | d$^3$ | d$^5$ | d$^6$ | d$^7$ | d$^8$ | d$^9$ |
| $\Delta E(1)$, kJ/mol | 33 | −128 | −268 | −14 | −120 | 0 | −84 | 82 |
| No. of CO = $n$ | 6 | 6 | 6 | 5 | 5 | 4 | 4 | 3 |
| $\Delta E(1)/n$, kJ/mol | 5 | −21 | −45 | −3 | −24 | 0 | −21 | 27 |
| $S_{tot}$ of M(CO)$_n$ | 1.0 | 0.5 | 0 | 0.5 | 0 | 0.5 | 0 | 0.5 |
| $\Delta E(2)$, kJ/mol | * | * | * | −66 | −46 | −30 | −48 | −81 |
| No. of NMe$_3$ = $m$ | * | * | * | 2 | 1 | 1 | 1 | 0 |
| $S_{tot}$ of M(NMe$_2$) (NMe$_3$)$_m$ | * | * | * | 2.5 | 2.0 | 1.5 | 1.0 | 0.5 |

computing reaction energetics are given in the supplementary material.

We use CO as a sample neutral molecule for ligand exchange towards zero-valent metal, and evaluate the energetics of the following gas-phase exchange reaction where $3 \leq n \leq 6$,

Reaction 1 : M($^t$Bu$_2$DAD)$_2$ + $n$(CO)

$\rightarrow$ M$^0$(CO)$_n$ + 2($^t$Bu$_2$DAD).

This exchange reaction is moderately exothermic for the V, Cr, Fe, and Ni complexes, yielding −20 to −45 kJ/mol per CO (Table II), and so we expect these complexes to be reduced most easily to metal films. We suggest that it may be possible to trigger this reaction by physically bombarding the surface with a chemically inert co-reagent, like Ar plasma, or by chemical exchange with another neutral ligand such as benzene. By contrast, the reaction is energetically neutral for Ti, Mn, and Co and energetically unfavored for Cu (+27 kJ/mol per CO). An odd-even effect is thus visible in the M(II) series, perhaps indicating that reduction is less favored when there is residual spin. However, the spin-pairing picture will probably be different in the M−M bonding situation of an actual thin film.

In a similar way, we use the dimethylamino ligand (NMe$_2$)$^-$ (where Me = CH$_3$) to probe reactivity of the DAD complexes towards amines HNR$_2$, and evaluate $\Delta E$ of the following exchange reaction where $0 \leq m \leq 2$ neutral trimethyl amines are used to complete the coordination shell,

Reaction 2 : M$^{II}$($^t$Bu$_2$DAD)$_2$ + 2(NMe$_2$)$^-$ + $m$(NMe$_3$)

$\rightarrow$ M$^{II}$(NMe$_2$)$_2$(NMe$_3$)$_m$ + 2($^t$Bu$_2$DAD)$^-$.

It is computed that this reaction is moderately favored for all the M(II) complexes, indicating that DAD$^-$ is a weaker Lewis base than NMe$_2$$^-$. The reaction energy decreases in magnitude from left to right in the row (from $\Delta E(2) = $ −80 kJ/mol for Mn to −30 kJ/mol for Co, Table II), with an exceptionally high exothermicity for Ni (−48 kJ/mol) probably reflecting the relief of Jahn-Teller strain (see above). Amines should therefore be effective co-reagents for exchanging ligands with DAD complexes, especially for the early to mid transition metals. It is not however clear how such ligand exchange would

lead to metal ALD, as it does not exploit the non-innocent behavior of DAD. One possibility is that the resulting amido fragment would auto-decompose to a nitride. By the same reasoning, co-reagents containing oxygen are likely to lead to metal oxides, as indeed reported for Ni(DAD)$_2$ with formic acid.[56]

This gas-phase study has revealed the importance of the magnetic contribution to binding in the transition metal DAD complexes, and hence to structure and reactivity. Expanding the model to compute surface intermediates during the actual ALD process will therefore also require the careful inclusion of spin. Until this is done, conclusions about the ALD mechanism and best choice of co-reagents are speculative. The gas-phase data suggest that displacement of DAD by neutral ligands may be a fruitful approach for ALD of V, Cr, Fe, and Ni, while Brønsted acidic amines may be viable co-reagents for Mn, Fe, Ni, and perhaps Co. Another approach may be to physically displace neutral DAD from the metallic surface, e.g., by Ar plasma, but this would lead to an abbreviated cycle and correspondingly low growth rate, as a surface saturated with Ar atoms cannot be expected to form (i.e., steps 2b and 1a).

## V. CONCLUSION

In this paper we have examined various processes for the ALD of metals according to the role played by each reagent in supplying metal cations, supplying electrons, saturating the surface with ligands, and eliminating those ligands. Some of the mechanisms are those proposed through experiment, augmented with computed structures and energetics. Some mechanisms are based on first principles DFT calculations of reaction intermediates and transition states, which yield detailed information about which of the possible mechanistic routes are thermodynamically and kinetically favoured. For model systems of the size and complexity required to describe ALD, the laboriousness of these calculations poses a substantial bottleneck, since automated approaches for transition state searching frequently do not work. Problems also remain with the accuracy of total energies at transition states from Kohn Sham DFT and more accurate approaches that are competitive in terms of CPU time are currently lacking.

**CLASSIFICATION OF PROCESSES FOR METAL ALD ACCORDING TO MECHANISM**

| Metal precursor | | Co-reagent | | By-products | Examples | Section |
|---|---|---|---|---|---|---|
| M | X | M² | Y | | | |
| Reducible cation | Oxidisable Brønsted base | None | Oxidising agent for removing X & oxidising M | HX & oxidation product of X | Noble metals only | IV.B |
| Cation for reduction | Redox inert Brønsted base or reducible | None | H or H- is reducing agent by coupling to X | XY=HX or hydrogenation product of X | $H_2$ or organic; abbreviated cycle | III.A |
| Cation for reduction | Reducing agent by coupling with Y | Co-deposited as alloy or M²=M | Redox inert anion | XY | Hypersilyl | IV.A |
| Cation for reduction | Redox inert anion for exchange to M² | Redox inert cation | Reducing agent when exchanged to M | M²X & oxidation product of Y | Transmetallation / metal hydrides | III.B |
| Cation for reduction | Redox inert anion for donation to M² | Oxidisable cation to accept X | Inert spectator anion | M²XY | Metallocene proposal | III.C |
| Zero-valent M | Neutral or non-innocent ligand | None | Neutral species to displace X but unstable with M | X & Y | Diazadienyl or zero-valent Ru; abbreviated cycle | IV.C |
| Zero-valent M | Neutral or non-innocent ligand | Redox inert Lewis acid to accept X | Inert spectator anion | M²XY | Diazadienyl or zero-valent Ru | IV.C |

Colour code:

| Reducing agent; electron donor | Electron donor if oxidised | Redox inert | Electron acceptor if reduced | Oxidising agent; electron acceptor | Special case |
|---|---|---|---|---|---|

FIG. 9. Classification of metal ALD processes according to role played by each reagent.

Nevertheless, enough is known about the mechanism in most cases to suggest a cyclic mechanism, with each precursor reacting at the surface in a self-limiting way because (a) adsorbed co-reagent fragments become exhausted and (b) adsorbed precursor fragments render the substrate inert towards further precursor adsorption. This allows us to see what factors affect how much metal is deposited in each ALD cycle and we find that, in general, the growth rate depends on the saturating coverages of both co-reagent fragments and metal precursor fragments. Adsorption is via metal-metal bonding, which means partial oxidation of the substrate by the precursor. We highlight some cases, termed "abbreviated cycles," where the co-reagent cannot adsorb to the metal surface once precursor fragments are exhausted, which leads to low growth rates—typically 0.07–0.26 Å/cycle depending on metal valence. ALD processes based on $H_2$ or on zero-valent metal precursors are likely to show such abbreviated cycles.

We present a substantial body of computational work on copper ALD, spanning adsorption, choice of ligand, transmetallation mechanism, and alternative precursors. This includes new data on the potential decomposition of $Cu(acac)_2$ to copper oxide. Mechanistic information is also presented on metal ALD processes based on ligand-ligand coupling and on reducible oxides, such as those of noble metals. A computational study of the structure and reactivity of transition metal diazadienyl complexes is also presented, whose non-innocent behavior has yet to be fully exploited for metal ALD.

We are thus able to propose a classification of metal ALD processes according to whether the reducing agent is in the metal precursor or in the co-reagent, and whether the electrons come from the metal, ligand, or a non-organometallic reagent (Figure 9). It seems that all possible permutations have been proposed and most of them have been realized experimentally by at least one example. Organizing the concepts of metal ALD in this way may help in understanding the mechanism of existing processes and in designing new ones.

## SUPPLEMENTARY MATERIAL

See supplementary material for the methods used and the DAD results.

## ACKNOWLEDGMENTS

[1] T. Suntola and J. Antson, "Method for producing compound thin films," U.S. patent 4058430 (15 November 1977).

[2] V. Miikkulainen, M. Leskelä, M. Ritala, and R. L. Puurunen, J. Appl. Phys. **113**, 021301 (2013).

[3] D. J. H. Emslie, P. Chadha, and J. S. Price, Coord. Chem. Rev. **257**, 3282 (2013).

[4] T. J. Knisley, L. C. Kalataruge, and C. H. Winter, Coord. Chem. Rev. **257**, 3222–3231 (2013).

[5] R. L. Puurunen, J. Appl. Phys. **97**, 121301 (2005).

[6] S. D. Elliott and J. C. Greer, J. Mater. Chem. **14**, 3246 (2004).

[7] M. Shirazi and S. D. Elliott, Nanoscale **7**, 6311–6318 (2015).

[8] A. Zydor, V. G. Kessler, and S. D. Elliott, Phys. Chem. Chem. Phys. **14**, 7954–7964 (2012).

[9] W. Kaim, Inorg. Chem. **50**, 9752 (2011).

[10] K. Knapas and M. Ritala, Chem. Mater. **23**, 2766 (2011).

[11] A. B. Papandrew, C. R. I. Chisholm, R. A. Elgammal, M. M. Özer, and S. K. Zecevic, Chem. Mater. **23**, 1659 (2011).

[12] J. Hämäläinen, F. Munnik, M. Ritala, and M. Leskelä, Chem. Mater. **20**, 6840 (2008).

[13] J. Hämäläinen, E. Puukilainen, M. Kemell, L. Costelle, M. Ritala, and M. Leskelä, Chem. Mater. **21**, 4868 (2009).

[14] L. Wu and E. Eisenbraun, J. Vac. Sci. Technol., B: Microelectron. Nanometer Struct. **25**, 2581 (2007).

[15] X. Hu, J. Schuster, S. E. Schulz, and T. Gessner, Phys. Chem. Chem. Phys. **17**, 26892 (2015).

[16] M. Utriainen, M. Kröger-Laukkanen, L. S. Johansson, and L. Niinistö, Appl. Surf. Sci. **157**, 151 (2000).

[17] Q. Ma and F. Zaera, J. Vac. Sci. Technol., A **31**, 01A112 (2013).

[18] X. Hu, J. Schuster, S. E. Schulz, and T. Gessner, Microelectron. Eng. **137**, 23 (2015).

[19] E. Machado, M. Kaczmarski, P. Ordejón, D. Garg, J. Norman, and H. Cheng, Langmuir **21**, 7608 (2005).

[20] Y. Maimaiti and S. D. Elliott, J. Phys. Chem. C **119**, 9375 (2015).

[21] F. Zaera, Coord. Chem. Rev. **257**, 3177 (2013).

[22] G. Dey and S. D. Elliott, J. Phys. Chem. C **119**, 5914 (2015).

[23] Q. M. Phung, G. Pourtois, J. Swerts, K. Pierloot, and A. Delabie, J. Phys. Chem. C **119**, 6592 (2015).

[24] J. Kwon, M. Saly, M. D. Halls, R. K. Kanjolia, and Y. J. Chabal, Chem. Mater. **24**, 1025 (2012).

[25] Y. Maimaiti, M. Nolan, and S. D. Elliott, Phys. Chem. Chem. Phys. **16**, 3036 (2014).

[26] F. Zaera, Coord. Chem. Rev. **257**, 3177 (2013).

[27] M. M. Minjauw, J. Dendooven, B. Capon, M. Schaekers, and C. Detavernier, J. Mater. Chem. C **3**, 4848 (2015).

[28] P. Mårtensson, K. Larsson, and J.-O. Carlsson, Appl. Surf. Sci. **157**, 92 (2000).

[29] P. Martensson and J.-O. Carlsson, J. Electrochem. Soc. **145**, 2926–2931 (1998).

[30] I. K. Igumenov, P. P. Semyannikov, S. V. Trubin, N. B. Morozova, N. V. Gelfond, A. V. Mischenkoa, and J. A. Norman, Surf. Coat. Technol. **201**, 9003–9008 (2007).

[31] T. J. Knisley, T. C. Ariyasena, T. Sajavaara, M. J. Saly, and C. H. Winter, Chem. Mater. **23**, 4417 (2011).

[32] G. Dey and S. D. Elliott, RSC Adv. **4**, 34448 (2014).

[33] J. W. Klaus, S. J. Ferro, and S. M. George, Thin Solid Films **360**, 145 (2000).

[34] S. Klejna and S. D. Elliott, J. Phys. Chem. C **116**, 643–654 (2012).

[35] B. Vidjayacoumar, D. J. H. Emslie, S. B. Clendenning, J. M. Blackwell, J. F. Britten, and A. Rheingold, Chem. Mater. **22**, 4844–4853 (2010).

[36] B. H. Lee, J. K. Hwang, J. W. Nam, S. U. Lee, J. T. Kim, S.-M. Koo, A. Baunemann, R. A. Fischer, and M. M. Sung, Angew. Chem., Int. Ed. **48**, 4536–4539 (2009).

[37] G. Dey and S. D. Elliott, J. Phys. Chem. A **116**, 8893 (2012).

[38] G. Dey and S. D. Elliott, J. Phys. Chem. C **119**, 5914 (2015).

[39] Y. Maimaiti and S. D. Elliott, Chem. Mater. **28**, 6282–6295 (2016).

[40] G. Dey, J. S. Wrench, D. J. Hagen, L. Keeney, and S. D. Elliott, Dalton Trans. **44**, 10188 (2015).

[41] V. Pore, K. Knapas, T. Hatanpaa, T. Sarnet, M. Kemell, M. Ritala, M. Leskela, and K. Mizohata, Chem. Mater. **23**, 247–254 (2011).

[42] C. T. Sirimanne, M. M. Kerrigan, P. D. Martin, R. K. Kanjolia, S. D. Elliott, and C. H. Winter, Inorg. Chem. **54**, 7–9 (2015).

[43] G. Dey and S. Elliott, Theor. Chem. Acc. **133**, 1416 (2013).

[44] T. Aaltonen, P. Alén, M. Ritala, and M. Leskelä, Chem. Vap. Deposition **9**, 45 (2003).

[45] T. Aaltonen, M. Ritala, T. Sajavaara, J. Keinonen, and M. Leskelä, Chem. Mater. **15**, 1924 (2003).

[46] K. Knapas and M. Ritala, Chem. Mater. **20**, 5698 (2008).

[47] W. M. M. Kessels, H. C. M. Knoops, S. A. F. Dielissen, A. J. F. Mackus, and M. C. M. van de Sanden, Appl. Phys. Lett. **95**, 013114 (2009).

[48] S. D. Elliott, Langmuir **26**, 9179 (2010).

[49] C. K. Ande, S. D. Elliott, and W. M. M. Kessels, J. Phys. Chem. C **118**, 26683–26694 (2014).

[50] Q. Ma, H. Guo, R. G. Gordon, and F. Zaera, Chem. Mater. **23**, 3325 (2011).

[51] M. B. E. Griffiths, P. J. Pallister, D. J. Mandia, and S. T. Barry, Chem. Mater. **28**, 44 (2016).

[52] S.-H. Kim, ECS Trans. **41**, 19–23 (2011).

[53] T. J. Knisley, M. J. Saly, M. J. Heeg, J. L. Roberts, and C. H. Winter, Organometallics **30**, 5010 (2011).

[54] L.-M. Clement, and J. Lee, "Titanium bis diazadienyl precursor for vapor deposition of titanium oxide films," U.S. patent 20150072085 A1 (12 March 2015).

[55] A. Z. Bradley, J. S. Thompson, and K.-H. Park, "Copper (II) complexes for deposition of copper films by atomic layer deposition," U.S. patent 20080044687 A1 (21 February 2008).

[56] J. P. Klesko, M. M. Kerrigan, and C. H. Winter, Chem. Mater. **28**, 700–703 (2016).

[57] M. Kerrigan and C. H. Winter, 16th International Conference on Atomic Layer Deposition, Ireland, 2016.

[58] T. Pugh *et al.*, Inorg. Chem. **52**, 13719 (2013).

[59] N. Kaltsoyannis, J. Chem. Soc., Dalton Trans. **1996**, 1583.